Transonic Shock-Free Aerofoil Design by an Analytic Hodograph Method

J.W. Boerstoel* and G.H. Huizing†
National Aerospace Laboratory (NLR), Amsterdam, The Netherlands

A design method for transonic shock-free aerofoils using hodograph theory is sketched. The method is based on the approximate solution of Tricomi boundary value problems for the elliptic-hyperbolic hodograph equations of transonic aerofoil flows on a two-sheeted hodograph surface. Special attention is paid to a numerical approximation method generating nearly always closed aerofoils. The use of the computer programs in an aerodynamic design process is illustrated by an example. Several examples of computed aerofoils (some of them advanced) demonstrate that the method is flexible and powerful.

I. Introduction

IN 1969 it became clear that the hodograph method for profile design used at NLR should be extended to permit the calculation of advanced aerofoils. The class of transonic shock-free quasi-elliptical hodograph aerofoils of Nieuwland[1] developed in the 1962-1970 period became too limited (from an engineering point of view) because, for practical reasons, the number of parameters for control of the aerofoil shapes had to be restricted to too small a number.‡

The difficulties originate from the fact that the method transforms incompressible flows around aerofoil-like shapes into transonic flows around aerofoils. Therefore, this approach should not be used when a design method for arbitrary transonic shock-free aerofoils is desired.

A calculation method for the design of transonic shock-free aerofoils of arbitrary shape can also, at least in principle, be based on the solution of Tricomi boundary value problems for the mixed elliptic-hyperbolic hodograph equations by constructive approximation methods (see, e.g., Ref. 4). Such a calculation method can only be successful from an engineering point of view if the class of aerofoils that can be generated is large, and thus if the boundaries can be chosen sufficiently general. Since suitable solution methods were not available, many questions concerning the existence of solutions, the approximation method, convergence of sequences of approximations and numerical performance (speed and accuracy) of algorithms had to be considered and answered (at least partially).

Tricomi boundary value problems can in principle be approximately solved by various methods and a choice had to be made in this respect. The methods considered were finite difference techniques and truncated series of particular solutions. Because the approach with truncated series would permit the use of the vast experience gathered at NLR with the Lighthill-Nieuwland hodograph theory for quasi-elliptical aerofoils,[1] this approach was preferred. Moreover, it could be expected that ultimately, accuracy problems could be better kept under control with this approach.

Having selected this approach, two major problems had to be faced. The first was the method of determining the coefficients of the particular solutions in the truncated series, a reliable method not being available. Using mathematical model studies[10] (the solution of Dirichlet boundary value problems for Laplace's equation), this problem could be satisfactorily solved. A second problem was to guarantee that in supersonic regions of the flow, the aerofoil contour would be a continuous curve. It may be argued from a mathematical point of view that this is not necessarily the case. It will be shown that this problem has also been solved satisfactorily in a practical sense.

The first purpose of this paper is to outline some new mathematical concepts that were used in the computation method. A second purpose is to illustrate the use of the corresponding computer program set in an aerodynamic design process and to present examples of computed aerofoils.

Presented as Paper 74-539 at the AIAA 7th Fluid and Plasma Dynamics Conference, Palo Alto, California, June 17-19, 1974; submitted July 8, 1974; revision received April 29, 1975. The results presented were obtained in investigations performed under contract with the Netherlands Agency for Aerospace Programs (NIVR).

Index category: Aircraft Aerodynamics (including Component Aerodynamics); Subsonic and Transonic Flow.

*Senior Mathematician. Member AIAA.

†Senior Systems Analyst.

‡Nieuwland's class of quasi-elliptical aerofoils contains, in fact, about fifty parameters; nine parameters have been investigated, the other parameters are given fixed values because systematic variation would be an impossible task. The same argument applies to Takanashi's method,[2] that was later developed. The hodograph method of Korn and Garabedian[3] has the same drawback. In order to be able to compute a large class of aerofoils they increased the number of parameters to over 70, by adding special solutions. However, the determination of the parameters is then very difficult because these have to be balanced extremely carefully.

II. Theory

Sketch of Tricomi Boundary Value Problem

It is known that transonic shock-free aerofoils in potential flows can be represented by solutions of a linear partial differential equation of elliptic-hyperbolic type for the stream function $\tilde{\Psi}$:

$$\tilde{L}\,\tilde{\Psi}(M,\Theta)=0 \tag{1}$$

where M is the local Mach number and Θ the local flow angle. Such solutions are found to be defined on a two-sheeted (M, Θ) surface with a point (M^*, Θ^*) as branch point. The (M, Θ) surface is the hodograph surface.

Let us first sketch the structure of the solutions in terms of the hodograph variables and the relation between the physical plane of the flow around the aerofoil and the hodograph surface (see also Fig. 1).

1) (M, Θ) are polar variables on the hodograph surface, with M as radial variable.

2) The hodograph surface may be divided into two sheets by a cut that begins at the branch point (M^*, Θ^*) and extends

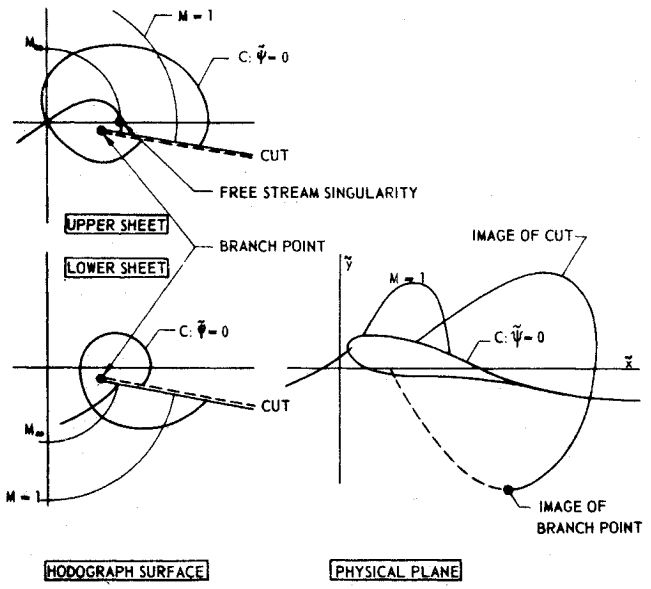

Fig. 1 Structure of hodograph of shock-free transonic flow.

outward along the radius $\Theta = \Theta^*$. We will distinguish between the sheets by calling them upper and lower sheet.

3) The image $\tilde{\Psi} = 0$ of the aerofoil on the hodograph surface is a closed curve C encircling the branch point. The exterior of the aerofoil in the physical plane maps onto the interior of the aerofoil image C on the hodograph surface.

4) The stream function $\tilde{\Psi}$ of the flow has a freestream singularity of known type at infinity in the physical plane, and thus at a point $(M_\infty, 0)$ on one of the sheets of the hodograph surface (M_∞ freestream Mach number). We will define that the sheet containing the freestream point $(M_\infty, 0)$ is the upper sheet.

5) The freestream line $\tilde{\Psi} = 0$ that extends in the physical plane from the front stagnation point to infinity upstream corresponds to a curve on the upper sheet from the origin to $(M_\infty, 0)$ where $\tilde{\Psi}$ has its freestream singularity. Similarly, the freestream line $\tilde{\Psi} = 0$ from the tail point downstream to infinity maps onto a curve connecting the tail point image on the lower sheet with $(M_\infty, 0)$ on the upper sheet.

6) The mapping from the hodograph surface (M, Θ) to the physical plane $\tilde{z} = \tilde{x} + i\tilde{y}$ is given by a relation of the form

$$\tilde{z}(M,\Theta) = \tilde{M}\tilde{\Psi}(M,\Theta) \tag{2}$$

where $\tilde{M}$ is a known linear operator (see Ref. 5, article 17.3) that need not be specified further here.

The Tricomi boundary value problem for transonic shock-free aerofoil design can now be sketched. Assume that the aerofoil image C is given, together with the freestream Mach number M_∞ and the location of the branch point (M^*, Θ^*). Assume also that the freestream singularity in the stream function has been split off by putting

$$\tilde{\Psi} = \tilde{\Psi}_b + \tilde{\Psi}_a \tag{3}$$

where $\tilde{\Psi}_b$ is a given basic stream function having the desired freestream singularity and satisfying the partial differential equation $\tilde{L}\,\tilde{\Psi}_b = 0$. The stream function $\tilde{\Psi}_a$ must then also satisfy inside the aerofoil image C the partial differential equation

$$\tilde{L}\tilde{\Psi}_a = 0 \tag{4}$$

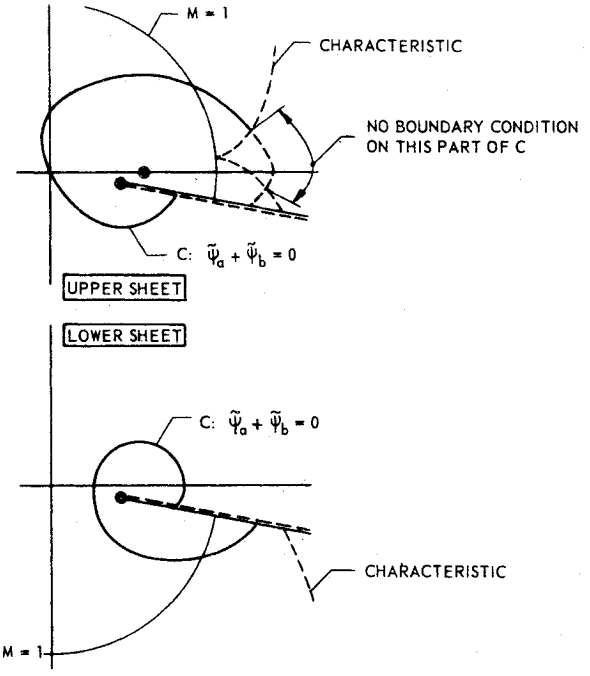

GIVEN: M_∞, (M^*, θ^*), $\tilde{\psi}_b$ AND C

REQUIRED: $\tilde{L}\,\tilde{\psi}_a = 0$

$\tilde{\psi}_a + \tilde{\psi}_b = 0$ ON C

Fig. 2 Tricomi boundary value problem.

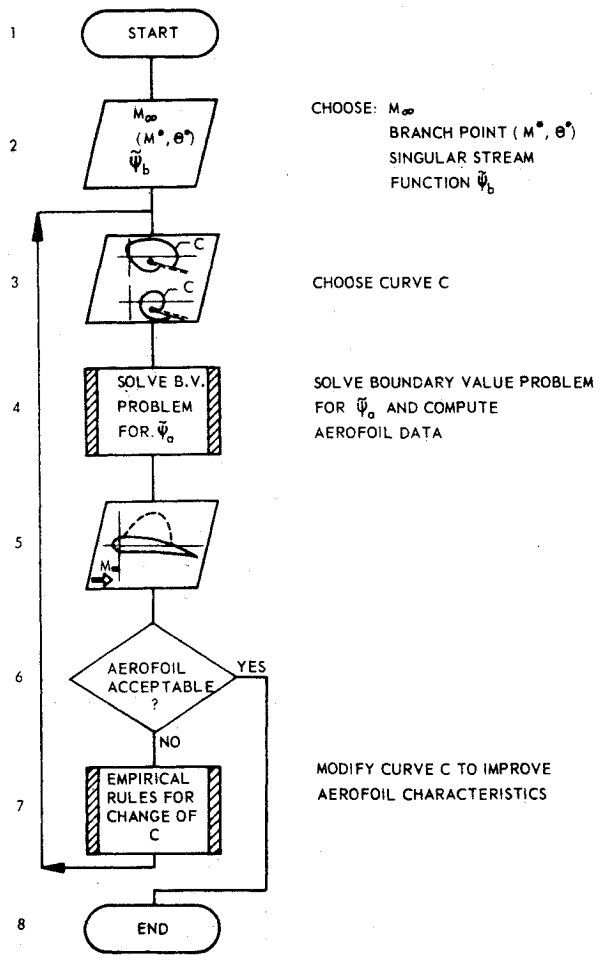

Fig. 3 Aerodynamic design process.

Furthermore, $\tilde{\Psi}_a$ has to satisfy on the aerofoil image C the relation

$$\tilde{\Psi}_a + \tilde{\Psi}_b = 0 \tag{5}$$

This implies that a boundary value problem for the stream function $\tilde{\Psi}_a$ has to be solved if $\tilde{\Psi}_a$ is not known. $\tilde{\Psi}_a$ may be called the additional stream function.

It is well known[4,6] that the boundary condition[5] cannot be prescribed on the entire boundary curve C. To avoid an overdetermined problem, the boundary condition should not be prescribed on a segment of curve C in the supersonic part of the hodograph surface, that lies between two characteristics of opposite class of the differential operator $\tilde{L}$ and coincide in some arbitrary point on the sonic line (see Fig. 2).

Tricomi Boundary Value Problem and Aerofoil Design

A transonic shock-free aerofoil may be determined by solving first a Tricomi boundary value problem for the additional stream function $\tilde{\Psi}_a$ for a given freestream Mach number, branch point (M^*, Θ^*), basic stream function $\tilde{\Psi}_b$, and aerofoil image C. Next the aerofoil contour in the physical plane is determined from Eq. (2) and the pressure distribution in the shock-free flow is obtained.

The aerofoil designer is thus confronted with an algorithm having as input a few parameters (M_∞, M^*, Θ^* and those parameters that define the basic stream function $\tilde{\Psi}_b$ and an assumed aerofoil image C on the hodograph surface, and as output the aerofoil geometry and the corresponding pressure distribution. He may then iterate to a transonic shock-free aerofoil having required physical properties (Fig. 3). The required physical properties concern for example the pressure distribution (peaky or nonpeaky, rear-loading, pressure gradients) and desired geometrical properties (nose shape, tail shape, location of curvature peaks, etc.).

It will be evident that the design process is only useful if, from the engineering point of view, 1) the position of the boundary contour can be varied within sufficiently wide limits; 2) the empirical rules are simple; and 3) the numerical performance (speed and accuracy) of the algorithm is sufficient.

Choice of Singular Solution $\tilde{\Psi}_b$

A singular solution $\tilde{\Psi}_b$ for transonic flows can be derived from a singular solution for incompressible flows with the Lighthill-Nieuwland transformation technique.[1,7] A survey of the principles of the technique is given by Yoshihara.[8]

The singular solution for incompressible flows is defined as the sum of five terms:

$$\Psi_b \equiv Im\phi_b \tag{6}$$

$$\phi_b \equiv \frac{i\Gamma}{2\pi}\{\tfrac{1}{2}\xi_\infty^{-2}\zeta^{-1}\phi_{dip} + \phi_{ln}\} + \phi_e - \phi_{ec} - \phi_{bc} \tag{7}$$

where Γ is the circulation of the flow, ζ^* the complex conjugate velocity in the branch point of the hodograph of the incompressible flow, and the other variables are defined below (ζ being the complex conjugate velocity of incompressible flow):

$$\xi \equiv (1-\zeta/\zeta^*)^{\frac{1}{2}} \tag{8}$$

$$\xi_\infty \equiv (1-1/\zeta^*)^{\frac{1}{2}} \tag{9}$$

$$\phi_{dip} \equiv (1-\frac{\xi}{\xi_\infty})^{-1} \tag{10}$$

$$\phi_{ln} \equiv \int^{(-\zeta)} \phi_{dip}\,\mathrm{d}(-\zeta) = -\ln(1-\frac{\xi}{\xi_\infty}) - \frac{\xi}{\xi_\infty} \tag{11}$$

$$\phi_e \equiv \xi(1-\epsilon\zeta/\zeta^*)^{-\frac{1}{2}} + \xi^{-1}(1-\epsilon\zeta/\zeta^*)^{\frac{1}{2}} \tag{12}$$

$$\phi_{ec} \equiv (1-\epsilon)^{\frac{1}{2}}\xi^{-1} \tag{13}$$

$$\phi_{bc} \equiv (i\Gamma\xi/2\pi\xi_\infty) \tag{14}$$

It can be seen that the terms with ϕ_{dip} and ϕ_{ln} are intended to guarantee that Ψ_b has the desired singular behavior at the freestream singularity in incompressible flow. The other terms are chosen in such a way that the basic solution becomes that of the flow over a thin ellipse-like shape. Further, it can be seen that the two-sheeted nature of the hodograph surface has been taken into account by removing the branch point by a conformal mapping from the hodograph surface to a ξ plane. There are still other reasons for the splitting up into the five terms which are of a mathematical technical nature; they will be discussed in Ref. 9.

The singular solution for transonic flows is derived from the incompressible singular solution using (with some simplifying modifications[9]) the Lighthill-Nieuwland transformation technique for each of the five terms. The final result is a large number of complicated series representations for $\tilde{\Psi}_b$ and $\tilde{z}_b$ which are one-valued on a two-sheeted hodograph surface for transonic flows, with some point (M^*, Θ^*) as a branch point.

Choice of Regular Solution $\tilde{\Psi}_a$

The Tricomi boundary value problem will be solved approximately by representing $\tilde{\Psi}_a$ by a finite sum of linearly independent solutions $\tilde{\Psi}_{an}$:

$$\tilde{\Psi}_a = \sum_{n=1}^{N} c_n \tilde{\Psi}_{an} \tag{15}$$

$$\tilde{L}\tilde{\Psi}_{an} = 0, \qquad n \neq 1\ (1)N \tag{16}$$

The partial differential equations are then automatically satisfied (by linearity of $\tilde{L}$) while the coefficients c_n are available to approximately satisfy the boundary condition. They will be determined from the boundary condition by a special method.

When the coefficients c_n in the additional stream function have been found the physical plane variable, $\tilde{z}$ can be found with the linear operator $\tilde{M}$:

$$\tilde{z} = \tilde{M}\tilde{\Psi} \tag{17a}$$

$$\tilde{z} = \tilde{M}\tilde{\Psi}_b + \sum_{n=1}^{N} c_n \tilde{M}\tilde{\Psi}_{an} \tag{17b}$$

The regular solutions $\tilde{\Psi}_{an}$ with corresponding formulas for $\tilde{M}\,\tilde{\Psi}_{an}$ for transonic flows are also defined from corresponding regular solutions for incompressible flow by the Lighthill-Nieuwland transformation technique.[7] For incompressible flows we chose as incompressible regular solutions the real and imaginary parts of the expressions

$$\xi^m = (1-\zeta/\zeta^*)^{\frac{1}{2}m} \tag{18}$$

The final results are series representations for the regular solutions $\tilde{\Psi}_{an}$ for the transonic flows and for the corresponding $\tilde{M}\,\tilde{\Psi}_{an}$. These series representations are one-valued on the two-sheeted hodograph surface for transonic flows. Each $\tilde{\Psi}_{an}$ is an exact solution of $L\,\tilde{\Psi}_{an} = 0$.

III. Numerical Solution of Tricomi Boundary Value Problem

The Tricomi boundary value problem for the regular solution $\tilde{\Psi}_a$ can be approximately solved by suitably deter-

mining the coefficients c_n in Eq. (15). Our numerical experiments revealed that all available standard methods for the determination of these coefficients failed to be successful. The problem was that the aerofoils (in particular in the subsonic parts) were usually not closed. Some more details will be given when discussing numerical results of Fig. 8 in Sec. VII.

The point to be observed is that making $\tilde{\Psi}_a + \tilde{\Psi}_b$ approximately zero on the assumed aerofoil image C is not essential. What is important is that the curve C', where the condition $\tilde{\Psi}_a + \tilde{\Psi}_b = 0$ is satisfied exactly (this curve lies close to the assumed aerofoil image C in a good approximate solution) must be closed. For it can be shown that the aerofoil (which corresponds to the curve C' and not to the assumed aerofoil image C) is then also closed. On the other hand, if C' is not closed, the aerofoil will not be a closed curve either.

The mathematical model studies[10] mentioned in the Introduction have revealed that a suitable method for the determination of the coefficients c_n, giving (nearly always) closed aerofoil images C' near the assumed aerofoil image C, consists of the minimization of a special error functional that measures the difference between C and C' (see Fig. 4; note the removal of the branch point of the hodograph surface by the mapping to a $\tilde{\xi}$ plane):

$$E = \oint w(s)\ \{n(s)\}^2 ds \tag{19}$$

where $w(s)$ is a given nonnegative weight function (usually $\equiv 1$), and $n(s)$ the distance between the curves measured along normals to the assumed aerofoil image C. This error functional is discretized by the trapezoidal rule, and the distances $n(s)$ are computed from linear approximations to the stream function as indicated in Fig. 5. The result is

$$E \cong \sum_{k=1}^{K} w_k \left[\frac{\tilde{\Psi}_{ko} + \tilde{\Psi}_{ki}}{\tilde{\Psi}_{ko} - \tilde{\Psi}_{ki}} \right]^2 n_{dk}^2 \tfrac{1}{2} (\Delta_k + \Delta_{k-1}) \tag{20}$$

where Δ_k are the arc lengths between successive given points on C, n_{dk} are given distances on normals to C in the given points on C, and $\tilde{\Psi}_{ko}$ and $\tilde{\Psi}_{ki}$ are values of $\tilde{\Psi}$ indicated in Fig. 5. Minimization of this error functional by varying the coefficients c_n using a standard method[11] gives satisfactory results.

IV. Accuracy of Computed Final Aerofoil Data

When the coefficients c_n have been determined, the aerofoil can be determined by computing a sequence of points. In each point the equation $\tilde{\Psi}(M, \Theta) = 0$ is solved at a chosen fixed value of M for Θ by the regula falsi. Next, $\tilde{z}(M, \Theta)$ and the aerofoil curvature are computed from analytically differentiated series expansions for the derivatives of the stream function $\tilde{\Psi}$. The series representations for $\tilde{\Psi}$ and $\tilde{z}$ are summed either directly or with a convergence accelerator (the complex ϵ algorithm).

Because the infinite series representations for $\tilde{\Psi}$ and $\tilde{z}$ are exact solutions of the hodograph equations, the only errors in the final results are due to truncation of the regula falsi process and to truncation of the series expansion when summing directly. When the series are summed by the ϵ algorithm, errors arise that can be considered to be of stochastical nature; the magnitude of these errors can be easily estimated and controlled. Other data (Chaplygin functions, coefficients in series representations) are computed to such a high precision that they cannot affect the precision of the final data.

The accuracy of the aerofoil contour data is 10^{-4} to 10^{-5} of the chord (without smoothing interpolation operations). If desired, it is possible to compute coordinates, slopes, and curvatures in about 400 points. This is sufficient for engineering purposes.

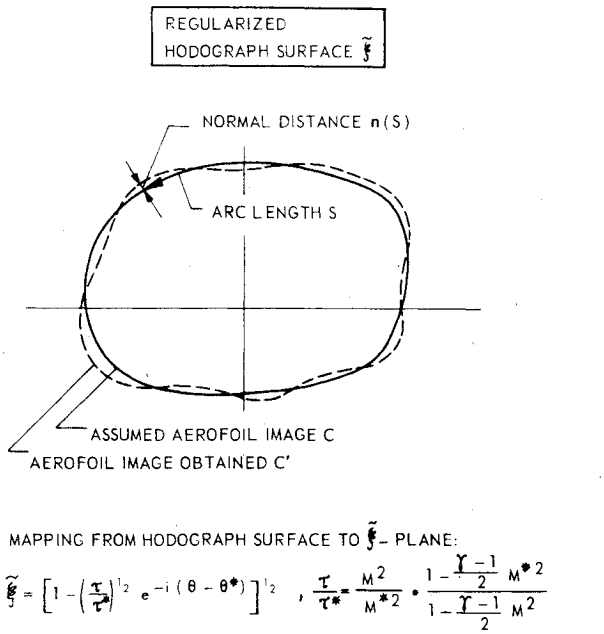

Fig. 4 Definition of normal distance $n(s)$ on regularized hodograph surface [Eq. (19)].

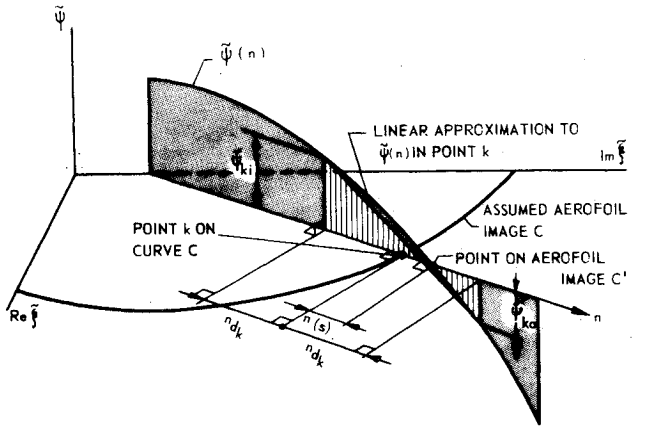

Fig. 5 Definition of variables in approximate error norm.

V. Use of the Computer Program Package

The computer program package consists of nine ALGOL programs performing calculations and data transfer. The package makes use of one tape and four permanent files for data to be retained. Sixteen files are used for input and output of data.

For a specific aerofoil design the package has to be operated in three stages:

1) About seven parameters that determine the basic stream function $\tilde{\Psi}_b(M_\infty, M^*, \Theta^*$, flow circulation Γ, ϵ, etc.) have to be determined in such a way that the hodograph seems a reasonable starting point to obtain the desired aerofoil. This is done by computing lines $\tilde{\Psi}_b = 0$ in the regularized hodograph plane $\tilde{\xi}$ defined in Fig. 4. (The choice of $\tilde{\Psi}_b$ is sometimes checked by computing explicitly the aerofoil-like shape defined by the lines $\tilde{\Psi}_b = 0$).

2) An assumed image C of the aerofoil is then defined on the regularized hodograph surface $\tilde{\xi}$, the corresponding coefficients c_n are computed, and the aerofoil image C' where $\tilde{\Psi} = 0$ is estimated.

3) When the aerofoil image C' lies close enough to the assumed aerofoil image C, the aerofoil shape and other data corresponding to C' are computed.

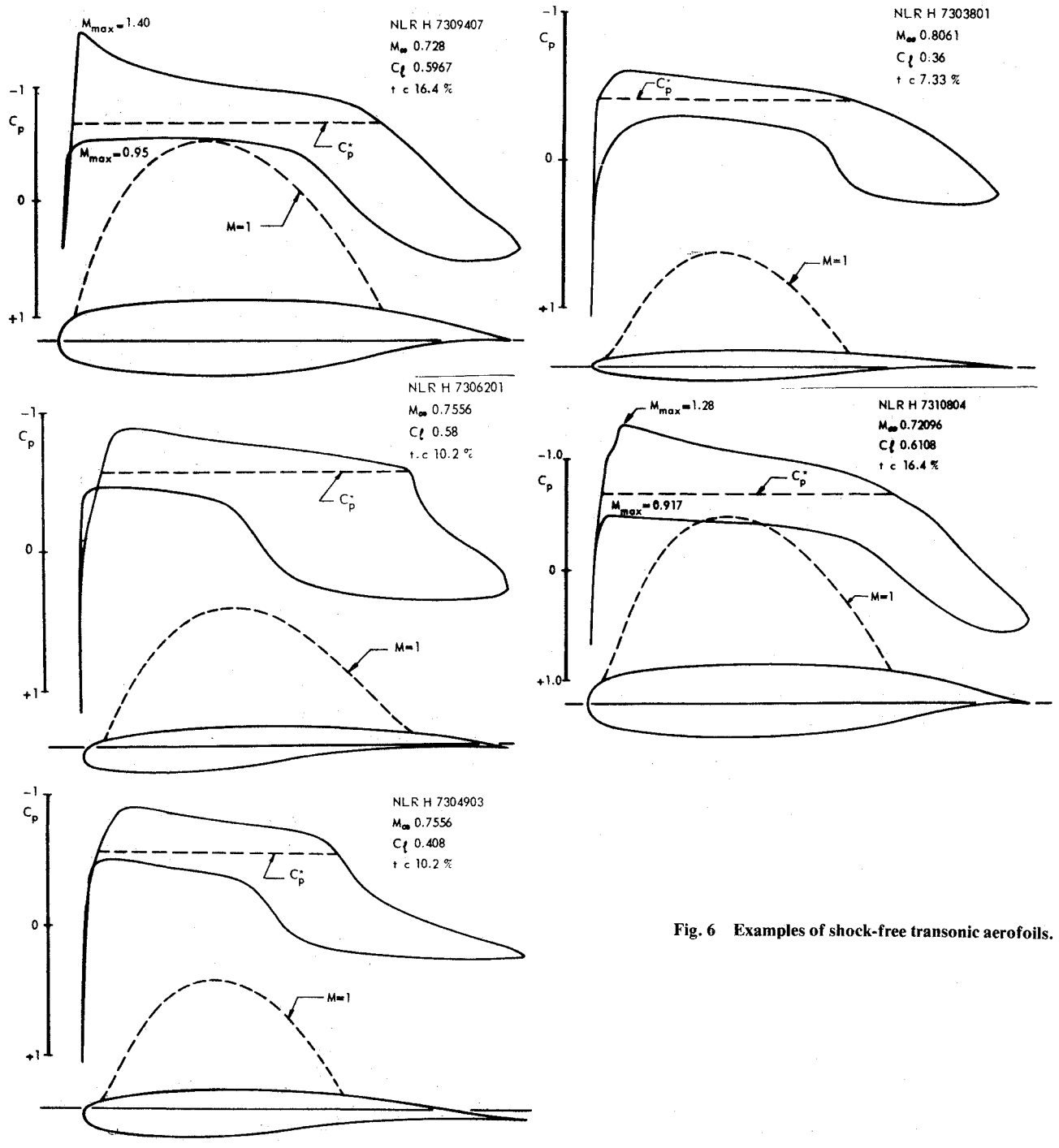

Fig. 6 Examples of shock-free transonic aerofoils.

When a particular aerofoil has to be designed, the input of the computation (the parameters that determine the singular solution $\tilde{\Psi}_b$ and the assumed aerofoil images C) has to be adjusted a few times in order to obtain an acceptable aerofoil. Experience has shown that—when the parameters of $\tilde{\Psi}_b$ have been fixed—usually only parts of the assumed aerofoil images C are redefined. This fact is used to save computation time by using data that were stored on tape in previous runs of the program set.

VI. Cost Experience

It was found that sufficient engineering accuracy can be achieved without trouble, and that computations with the program package can be well managed by aerodynamic engineers. (Only general knowledge of the mathematical theory and the numerical processes is needed.) Man-hour costs for aerofoil design are therefore considered to be acceptable.

For a typical calculation the system is run once to fix the parameters in the basic solution $\tilde{\Psi}_b$, once to fix the assumed aerofoil image C, and once for a calculation of the aerofoil shape (in about 130 points coordinates, slopes, curvatures, and pressures). On a CDC 6600 computer this would require about 1500 central processor seconds and 600 input-output seconds with an average of 26 K core store. The program set is operational on the smaller CDC Cyber 72 computer.

VII. Examples and Numerical Details

A survey of aerofoils computed until now is given in Fig. 6. The aerofoils cover a range of freestream Mach numbers, thickness ratios and lift coefficients, and have more or less rear loading. It may be concluded that from an aerodynamic

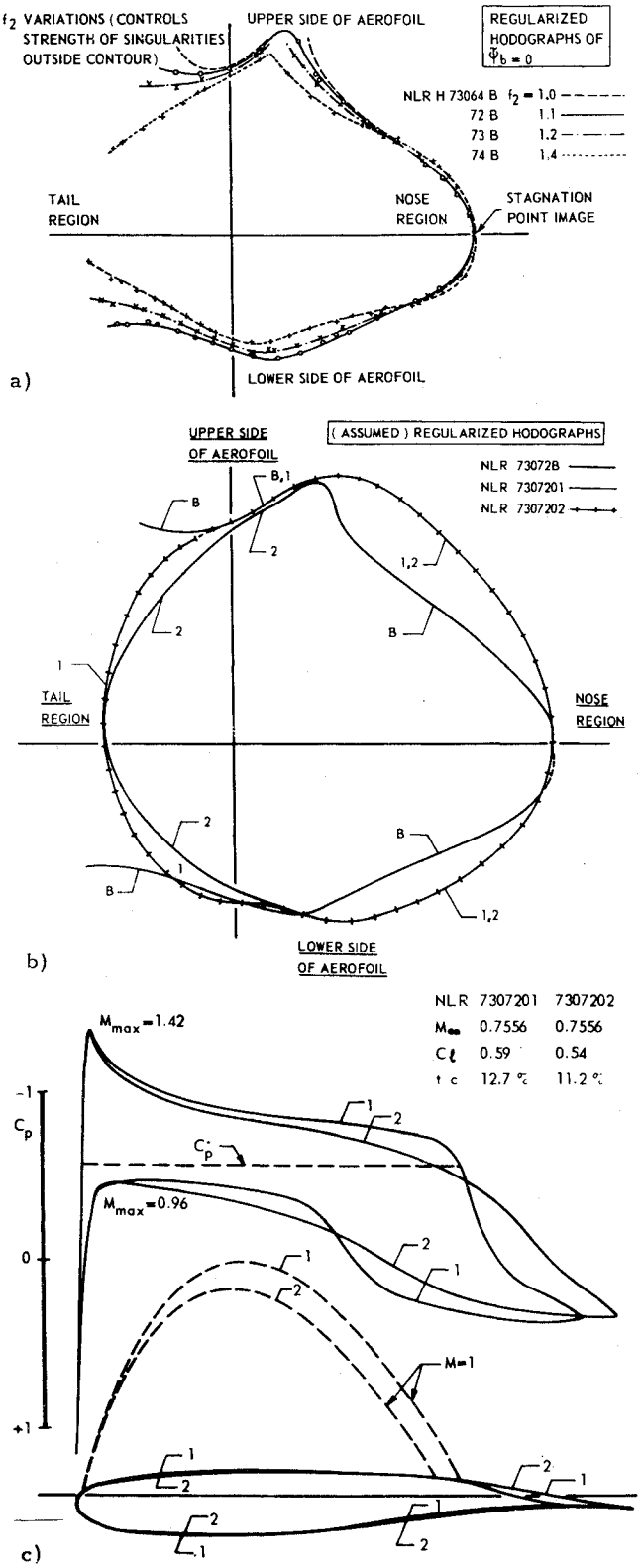

Fig. 7 Illustration of the design process of an aerofoil. a) Results of a parameter study for $\bar{\Psi}_b$. b) Choices of assumed aerofoil images for two aerofoils. c) Examples of transonic shock-free aerofoils.

point of view, a sufficiently wide range of interesting aerofoils can be computed.

An illustration of the design process of an aerofoil is given in Fig. 7. Results of a parameter study for singular solution $\bar{\Psi}_b$ are presented in Fig. 7a. The heavily drawn line represents the $\bar{\Psi}_b = 0$ line of the singular solution ultimately chosen. Figures 7b and 7c show the optimization to an assumed aerofoil image C giving an acceptable aerofoil shape.

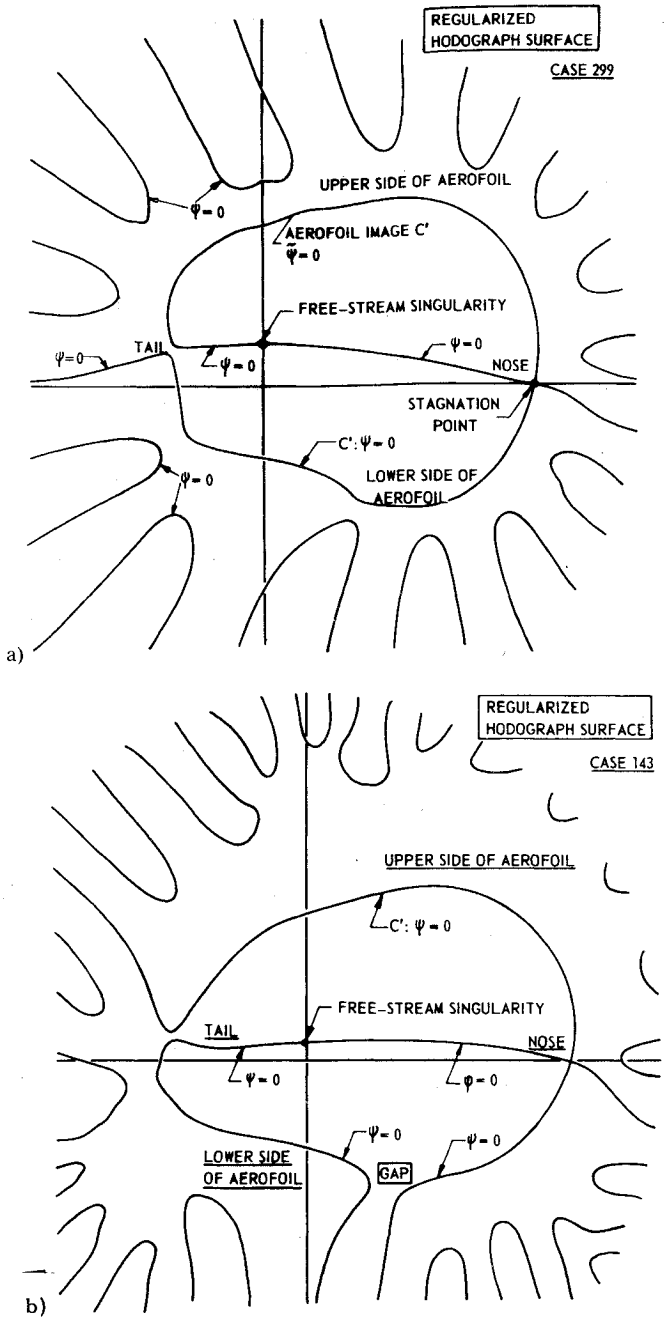

Fig. 8 Patterns of streamlines $\Psi = 0$ (incompressible flow): a) acceptable, b) meaningless.

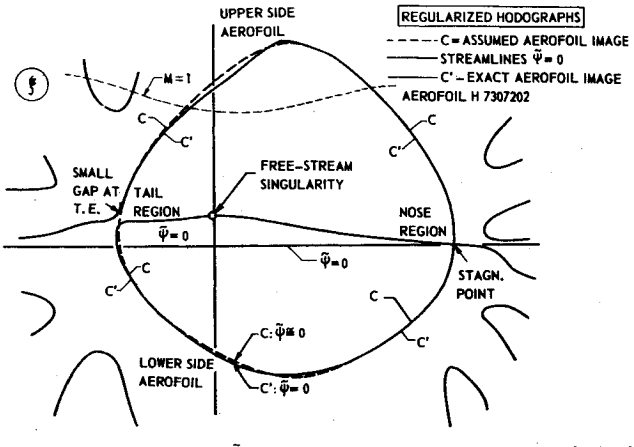

Fig. 9 Pattern of lines $\bar{\Psi} = 0$ for transonic aerofoil on regularized hodograph surface.

Some numerical details are shown in Figs. 8 and 9. Figure 8 shows (for the case of incompressible flow) what can be wrong with the aerofoil images C' on the regularized hodograph surface. Outside the aerofoil image C' ($\Psi=0$) there may be many other streamlines $\Psi=0$ that map into the interior of the aerofoil on the physical plane in a good approximate solution of the boundary value problem (Fig. 8a). However, in a meaningless approximate solution (Fig. 8b), the aerofoil image C' is not a closed curve. The situation may be wrong in quite more complicated ways; as indicated in Fig. 8b. In Fig. 9, acceptable results are shown for one of the transonic aerofoils of Fig. 6. In addition, the small differences between the input and output curves C and C' can be inspected. The error functional equation (19) suppresses possible gaps like those of Fig. 8b.

At the end of Sec. III it was mentioned that the boundary condition $\tilde{\Psi}=0$ on the assumed aerofoil image C should not be prescribed on a certain segment of C in the supersonic region of the flow. This can be realized by choosing some suitably chosen weights $w_k=0$ in expression (20). However, in practice this is often not necessary, and a choice $w_k \equiv 1$ is usually possible. This somewhat surprising procedure is possible for numerical reasons: in the supersonic regions $\tilde{\Psi}_b$ is "large" compared to $\tilde{\Psi}_a$ (in incompressible flow Ψ_b is large in corresponding regions due to the singularities of ϕ_e at $\zeta = \pm \zeta^*/\epsilon$; in transonic flow these singularities disappear, but the general behavior of $\tilde{\Psi}_b$ is similar to that for incompressible flow). Hence, in the supersonic regions the general character of the profile is determined by $\tilde{\Psi}_b$. For this purpose, too, ϕ_e (with its singularities at $\zeta = \pm \zeta^*/\epsilon$ outside the aerofoil images) has been incorporated in Ψ_b.

VIII. Conclusion

Based on hodograph theory, a computer program package has been developed that can be used for the aerodynamic design of shock-free transonic aerofoil sections. The program package provides final results of sufficient accuracy at acceptable costs and seems powerful and flexible enough to cover a wide range of engineering applications.

References

[1] Nieuwland, G.Y., "Transonic Potential Flow around a Family of Quasi-Elliptical Airfoil Sections, NLR-TR T-172, July 1967, National Aerospace Lab., Amsterdam, The Netherlands.

[2] Takanashi, S., "A Method of Obtaining Transonic Shock-Free Flow Around Lifting Aerofoils," private communication, 1971, National Aerospace Laboratory, Japan.

[3] Bauer, F., Garabedian, P., and Korn, D., "Supercritical Wing Sections," *Lecture Notes in Economics and Mathematical Systems,* Vol. 66, Springer Verlag, New York, 1972.

[4] Bers, L., *Mathematical Aspects of Subsonic and Transonic Gas Dynamics,* Wiley, New York, 1958.

[5] Von Mises, R., *Mathematical Theory of Compressible Fluid Flow,* Academic Press, New York, 1958.

[6] Manwell, A.R., *The Hodograph Equations,* Oliver and Boyd, Edinburgh, Scotland, 1971.

[7] Lighthill, M.J., "The Hodograph Transformation," in *Modern Developments in Fluid Dynamics, High Speed Flow,* Vol. 1, Clarendon Press, Oxford, England, 1953.

[8] Yoshihara, H., "Some Recent Developments in Planar Inviscid Transonic Airfoil Theory," AGARDograph no. 156, 1972.

[9] Boerstoel. J.W., "Transonic Shock-Free Aerofoil Design by Analytic Hodograph Theory," to be published.

[10] Boerstoel, J.W. and Huizing, G.H., "An Approximate Conformal Mapping Method Using Harmonic Polynomials," NLR TR 71019 U, 1971, National Aerospace Lab., Amsterdam, The Netherlands.

[11] Fletcher, R., "Generalized Inverse Methods for the Best Least Squares Solution of Systems of Non-Linear Equations," *Computer Journal,* Vol. 10, Feb. 1968, pp. 392-399.